

Modeling of ammonia-based wet flue gas desulfurization in the spray scrubber

Yong Jia, Qin Zhong[†], Xuyou Fan, Qianqiao Chen, and Haibo Sun

School of Chemical Engineering, Nanjing University of Science and Technology, Nanjing 210094, P. R. China
(Received 12 August 2010 • accepted 8 November 2010)

Abstract—A mathematical model of ammonia-based wet flue gas desulfurization process was developed based on the double film theory. The calculated results of the desulfurization system for two 220 t·h⁻¹ boilers per unit by this model were compared to that of corresponding measured data. It was found that the calculated results agree well with the measured data for the operating conditions of pH, liquid/gas ratio and SO₂ concentration. This model can provide predictions of the absorption performance of an ammonia-based wet flue gas desulfurization process and appears to be helpful for designing scrubbers for SO₂ absorption with ammonia absorbent.

Key words: Desulfurization, Ammonia, Spray Scrubber, Model, Simulation

INTRODUCTION

Sulfur dioxide (SO₂) in flue gas generated as a result of combustion of fossil fuel in, e.g., thermal power plants, industrial boilers, metallurgical furnaces and some chemical plants, is the main cause of global environmental problems such as air pollution and acid rain [1-3]. Many countries have therefore adopted strict regulations regarding SO₂ emissions. The world-wide concern about atmospheric pollution by SO₂ has led to the installation of flue gas desulfurization scrubbers on those plants. The most widely practiced method for sulfur dioxide control is based upon limestone or lime contact with flue gases in the form of aqueous slurry [4-7]. Typically, the by-product is either discarded in a landfill or converted into gypsum for use in wallboard and cement manufacturing. Disposal in a landfill requires a large initial capital investment as well as significant resources to maintain the landfill throughout the life of the plant. The value of the gypsum byproduct is low in China. Among the various flue gas desulfurization processes, the wet-type techniques using ammonia as an absorbent lead to efficient removal of SO₂ [8-11]. The ammonia-based wet flue gas desulfurization process is attractive as it results in the production of valuable ammonium sulfate without generating any other polluting by-products, according to the following reactions [3,11,12].



Use of ammonia reagent to absorb sulfur dioxide is also well known. Johnstone revealed the mechanism of ammonia-based wet flue gas desulfurization [13]. Saleem proposed an ammonia-based wet flue gas desulfurization process which was carried out in a single

vessel. The pilot plant experimental results show that the sulfur dioxide removal efficiency was very high and correlated with the liquid/gas ratio and pH. However, the oxidation of the sulfite was not complete [8]. In 1994, Saleem invented an ammonia-based wet flue gas desulfurization process which was carried out by first passing flue gas through a prescrubber, followed by passing the prescrubber gas through an absorber. The pilot plant experimental results indicated that the desulfurization efficiency was very high when the process of the invention utilized ammonia. The desulfurization efficiency varies with sulfur dioxide concentration and the ammonium sulfate by-product isolated as crystals from the process had a purity greater than 99.5% [9]. Borio proposed a process by which the flue gas was scrubbed in a countercurrent spray tower absorber with a spray of ammonium sulfate liquor. The ammonium sulfate liquor in the absorber system is passed into a separate reaction tank where ammonia and air are injected [10]. Using a stirred tank reactor, Gao performed experiments to study the gas-liquid absorption reaction between (NH₄)₂SO₃ and SO₂ for ammonia-based wet flue gas desulfurization [11].

Analysis of the literature revealed that there are few studies on the model of ammonia-based wet flue gas desulfurization and few models available indicating the performance of the spray scrubber of ammonia-based wet flue gas desulfurization systems. Therefore, it is meaningful to develop a model according to an actual operation mode to study the optimization of design and performance of ammonia-based wet flue gas desulfurization. In the present investigation, a mathematical model was developed to describe the desulfurization process of ammonia-based wet flue gas desulfurization according to the double film theory. The proposed model takes into consideration the pH value of the solution, liquid/gas ratio, flue gas velocity and SO₂ concentration.

MATHEMATICAL MODEL

An absorber that consists of absorption zone and slurry zone is the key component in wet flue gas desulfurization system. The sulfur dioxide is absorbed in the spray absorption zone by reacting with the ammoniacal scrubbing solution. The physical and chemical pro-

[†]To whom correspondence should be addressed.
E-mail: Zq304@mail.njust.edu.cn

cesses in the absorber include many complex factors such as size distribution of drops, velocity of drops, collision and coalescence between drops and heat exchange. It is difficult to describe all the processes in the absorber accurately by mathematical models. Accordingly, some assumptions were made as below:

- Flue gas is an ideal gas. In the falling process, the drops are considered to be a rigid ball in shape and a vertical line in trace.
- The radial concentration of SO_2 is constant in the spray scrubber, and the axial concentration varies with the height of the spray scrubber.
- The charge balance, chemical equilibrium and the ionic equilibrium in liquid drops are treated as instantaneous processes.
- The absorbed SO_2 gas undergoes a fast reaction with the absorber, which is complete within the liquid film. The oxidation of total sulfite in the absorption zone is neglected and all absorbed SO_2 is present as sulfite species.
- The system is isothermal and the heat exchange between the slurry and gas in the absorber is neglected.

1. Model Equations

In the absorption solution, there are nine different species, i.e., HSO_3^- , SO_3^{2-} , SO_4^{2-} , OH^- , H^+ , NH_4^+ , $\text{NH}_3 \cdot \text{H}_2\text{O}$, NH_3 and SO_2 , among which the following chemical equilibria take place:



By dividing the spray scrubber into small height incremental volumes (Fig. 1(a)), in each element, the variation of SO_2 concentration can be calculated according to steady-state mass balance equations [2]:

$$\frac{d}{dZ} \left(\frac{y}{1-y} \right) = \frac{k_g a (y - y_i)}{G(1-y_i)} \quad (12)$$

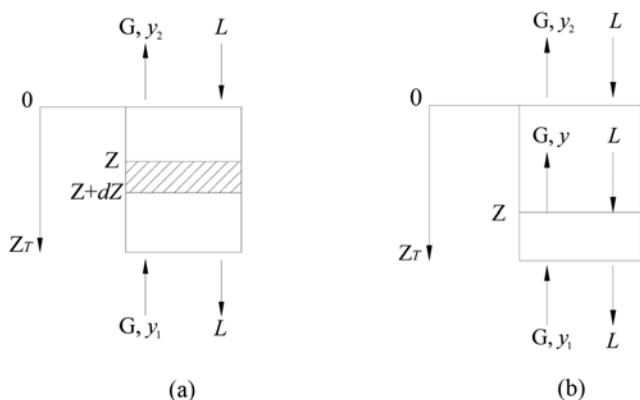


Fig. 1. Schematic diagram of mass balance.

Where:

$$y_i = \frac{p_{\text{SO}_2}^*}{p} \quad (13)$$

Boundary condition: $y(Z_T) = y_1$.

The contact area a can be determined by Eq. (12):

$$a = \frac{1}{3600} \cdot \frac{L}{\pi d_p^3} \cdot \pi d_p^2 \cdot \frac{dZ}{u_p} \quad (14)$$

The Sauter mean diameter of drops can be calculated by Eq. (16) [14]:

$$d_p = 133.0 \lambda \text{We}^{-0.74} \quad (15)$$

Where:

$$\text{We} = \frac{\rho_p u_p^0 \lambda}{\sigma} \quad (16)$$

Mass transfer coefficient in gas phase k_g is acquired by correlating Eqs. (17)-(20) [7,15-17].

$$\text{sh} = \frac{k_g d_p}{D_{\text{SO}_2} \text{Hp}} = 2 + 0.552 \text{Re}^{1/2} \text{Sc}^{1/3} \quad (17)$$

$$\text{Re} = \frac{d_p |u_p - u_g| \rho_g}{\mu_g} \quad (18)$$

$$\text{Sc} = \frac{\mu_g}{\rho_g D_{\text{SO}_2}} \quad (19)$$

$$D_{\text{SO}_2} = \frac{9.86 \times 10^{-3} T^{-1.75} \left(\frac{1}{M_{\text{air}}} + \frac{1}{M_{\text{SO}_2}} \right)^{0.5}}{p(V_{\text{air}}^{1/3} + V_{\text{SO}_2}^{1/3})^2} \quad (20)$$

The movement of falling drops in the absorption zone can be determined as Eqs. (21)-(22) [7,17,18]:

$$\frac{du_p}{dt} = g \left(\frac{\rho_p - \rho_g}{\rho_p} \right) - \frac{3}{4} \left(\frac{\rho_g (u_p - u_g)^2 C_{\text{drag}}}{\rho_p d_p} \right) \quad (21)$$

$$\int_0^{t_s} u_p dt = dZ \quad (22)$$

Moreover, the drag coefficient is achieved by Eq. (23) [7,17,18]:

$$C_{\text{drag}} = \frac{24}{\text{Re}} (1 + 0.125 \text{Re}^{0.72}) \quad (23)$$

It can be seen from Eqs (12)-(13) that the variation of y along the height of the spray scrubber can be calculated if $p_{\text{SO}_2}^*$ along the height of the spray scrubber is known.

$p_{\text{SO}_2}^*$ can be calculated according to vapor-liquid equilibrium equations. The charge balance of the solution can be written as:

$$[\text{H}^+] + [\text{NH}_4^+] = [\text{OH}^-] + [\text{HSO}_3^-] + 2[\text{SO}_3^{2-}] + 2[\text{SO}_4^{2-}] \quad (24)$$

According to Eqs. (6)-(11), Eq. (24) can be transferred into:

$$[\text{H}^+] + \frac{K_{hc} K_c P_{\text{NH}_3}^* [\text{H}^+]}{K_w} = \frac{K_w}{[\text{H}^+]} + \frac{K_{ha} K_{a1} P_{\text{SO}_2}^*}{[\text{H}^+]} + \frac{2K_{ha} K_{a1} K_{a2} P_{\text{SO}_2}^*}{[\text{H}^+]^2} + 2[\text{SO}_4^{2-}] \quad (25)$$

In Eq. (24), $P_{NH_3}^*$ is the equilibrium partial pressure of NH_3 , and it can be calculated according to the research results proposed by Johnstone [14]:

$$p_{NH_3}^* = N \frac{C(C-S)}{2S-C} \quad (26)$$

According to Eqs. (7)-(8), the distribution coefficient of each species of total sulfite (H_2SO_3 , HSO_3^- and SO_3^{2-}) can be described as follows:

$$\lambda_0 = \frac{[H^+]^2}{[H^+]^2 + K_{a1}[H^+] + K_{a1}K_{a2}} \quad (27)$$

$$\lambda_1 = \frac{K_{a1}[H^+]}{[H^+]^2 + K_{a1}[H^+] + K_{a1}K_{a2}} \quad (28)$$

$$\lambda_2 = \frac{K_{a1}K_{a2}}{[H^+]^2 + K_{a1}[H^+] + K_{a1}K_{a2}} \quad (29)$$

Taking the absorption of SO_2 and the volatilization of NH_3 into account, the pH level is usually controlled in the range of 5.5-6.2. Thus, the concentration of $NH_3 \cdot H_2O$ can be neglected. It can be seen from Fig. 2 that the distribution coefficient of H_2SO_3 is nearly zero when pH is above 5.0, and the distribution coefficient of H_2SO_3 is much lower than that of HSO_3^- and SO_3^{2-} . To simplify the calculation, the concentration of H_2SO_3 was neglected. Accordingly, Eq. (26) can be transformed into:

$$P_{NH_3}^* = 133.322 \times \frac{N \cdot [NH_4^+] \cdot ([NH_4^+] - [SO_3^{2-}] - [HSO_3^-])}{2([SO_3^{2-}] + [HSO_3^-]) - [NH_4^+]} \quad (30)$$

Thus, according to Eqs. (6)-(11), a nonlinear equation for correlation function between $[H^+]$ and $P_{SO_2}^*$ is acquired by correlating Eq. (25) and Eq. (30):

$$P_{SO_2}^* = \frac{[H^+]^3 - 2[SO_4^{2-}][H^+]^2 - K_w[H^+]}{(K_{ha}K_{a1}[H^+] + 2K_{ha}K_{a1}K_{a2})(1 - 133.322NK_{a2}K_{hc}K_c/K_w)} \quad (31)$$

The concentration of hydrogen ions $[H^+]$ along the height of the

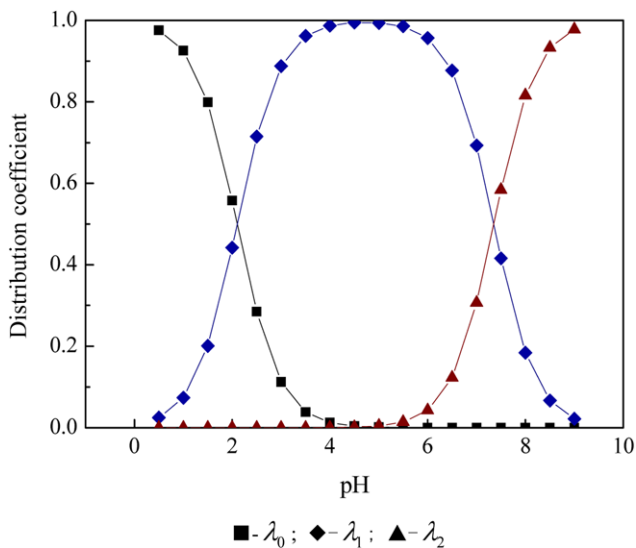


Fig. 2. Distribution coefficient of each species of total sulfite (Temperature=323.15 K).

spray scrubber should be calculated before the calculation of $P_{SO_2}^*$. Between the bottom and any cross section of the absorption zone (Fig. 1(b)), the mass balance of total sulfite can be written as follows:

$$M_{in,b} + M_{in,z} = M_{out,b} + M_{out,z} \quad (32)$$

Where:

$$M_{in,b} = G \cdot y_1 \quad (33)$$

$$M_{in,z} = L \cdot ([SO_2 \cdot H_2O] + [HSO_3^-] + [SO_3^{2-}]) = L \cdot K_{ha} P_{SO_2}^* \left(1 + \frac{K_{a1}}{[H^+]} + \frac{2K_{a1}K_{a2}}{[H^+]^2} \right) \quad (34)$$

$$M_{out,b} = G \cdot y_1 - \frac{G(1-y_1)y_2}{(1-y_2)} + L([SO_2 \cdot H_2O]_0 + [SO_3^{2-}]_0 + [HSO_3^-]_0) = G \cdot y_1 - \frac{G(1-y_1)y_2}{(1-y_2)} + L \cdot K_{ha} \cdot P_{SO_2,0}^* \left(1 + \frac{K_{a1}}{[H^+]_0} + \frac{2K_{a1}K_{a2}}{[H^+]_0^2} \right) \quad (35)$$

$$M_{out,z} = \frac{G(1-y_1)y}{(1-y)} \quad (36)$$

Combining Eqs. (32)-(36) yields:

$$Gy_1 + L \cdot K_{ha} P_{SO_2}^* \left(1 + \frac{K_{a1}}{[H^+]} + \frac{K_{a1}K_{a2}}{[H^+]^2} \right) = \frac{G(1-y_1)y}{(1-y)} + G \cdot y_1 - \frac{G(1-y_1)y_2}{(1-y_2)} + LI_0 \quad (37)$$

Where:

$$I_0 = K_{ha} \cdot P_{SO_2,0}^* \left(1 + \frac{K_{a1}}{[H^+]_0} + \frac{K_{a1}K_{a2}}{[H^+]_0^2} \right) \quad (38)$$

A nonlinear equation for the correlation function between $[H^+]$ and y is acquired by correlating Eq. (31) and Eq. (37):

$$y = \frac{f([H^+])}{1 + f([H^+])} \quad (39)$$

Where:

$$f([H^+]) = \frac{[H^+]^3 - 2[SO_4^{2-}][H^+]^2 - K_w}{G[H^+](1-y_1)(K_{ha}K_{a1}[H^+] + 2K_{ha}K_{a1}K_{a2})/L} \cdot \frac{K_{ha}[H^+]^2 + K_{ha}K_{a1}[H^+] + K_{ha}K_{a1}K_{a2}}{1 - 133.322N \frac{K_{hc}K_cK_{a2}}{K_w}} - \frac{I_0L}{G(1-y_1)} + E \quad (40)$$

$$E = y_2/(1-y_2) \quad (41)$$

Combining Eq. (12) and Eq. (39) yields:

$$\frac{d}{dZ} \left(\frac{y}{1-y} \right) = \frac{df([H^+])}{dZ} = \frac{df([H^+])}{d[H^+]} \cdot \frac{d[H^+]}{dZ} = \frac{k_y a (y - y_1)}{G(1-y_1)} \quad (42)$$

Eq. (42) can be transformed into:

$$\frac{d[H^+]}{dZ} = \frac{k_y a (y - y_1)}{G(1-y_1)} \cdot \left(\frac{df([H^+])}{d[H^+]} \right)^{-1} \quad (43)$$

The concentration of hydrogen ions along the height of the spray scrubber can be calculated by Eq. (43) and the concentration of SO_2 along the height of the spray scrubber can be calculated according to Eq. (39).

2. Numerical Method and Calculation Process

The spray scrubber was divided into small incremental volumes and computations were centered for each height incremental volume. In each volume, the pH value, the velocity of liquid drops, and the concentration of SO_2 and ions are all assumed to be of a uniform distribution. The pressure-swirl atomizers were used in the spray scrubber. The initial axial velocity of liquid drops was calculated to be 7.77 m/s according to equations proposed by Doumas [19]. According to Wu's investigation, the Sauter mean diameter was calculated to be 1.0×10^{-3} m when the liquid flow is of the design value [14]. Regarding the interaction effects among slurry drops, 1.8×10^{-3} m was taken as the diameter of the droplets. According to the operating conditions in ammonia-based wet FGD plants, the model input parameter of mass percent concentration of solution is 25% and the temperature is 323.15 K.

The calculation starts from the top of the spray scrubber. At the beginning of the calculation, the initial pH value and SO_2 outlet concentration y_2 were input to the solution as the known values. The concentration of $[\text{H}^+]$ along the height of the spray scrubber can be calculated according to Eq. (43). Then, the concentration of SO_2 y along the height of the spray scrubber was obtained by Eq. (39). The calculated value of SO_2 inlet concentration was compared with the given value of SO_2 inlet concentration. Repeating the above calculation steps, y_2 was adjusted until the absolute error of the calculated value of SO_2 inlet concentration was less than 0.001. Finally, the SO_2 removal efficiency can be expressed as: $\eta = (y_1 - y_2)/y_1$. In particular, the model parameters are presented in Table 1.

EXPERIMENTAL

All the experimental data in this paper were taken from an ammonia-based wet flue gas desulfurization system which is applied in a petrochemical works in Northwest China. The ammonia-based wet flue gas desulfurization system is similar to that proposed by Saleem [9]. The desulfurization process is carried out by first passing hot flue gas through a prescrubber, followed by passing the prescrubbed gas through the absorber. In the absorber, the flue gas flows upward and makes contact with the liquid drops sprayed from the

nozzles positioned on horizontal spray banks. The slurry circulates into the absorber over spray banks each of which has a dedicated recirculation pump. The clean flue gas leaves the absorber through the outlet duct after removing the entrained liquid drops.

In the desulfurization system, one spray scrubber is installed for two $220 \text{ t} \cdot \text{h}^{-1}$ boilers per unit. There are three spray banks in the absorber. Each spray bank is provided with forty spray nozzles. The design values of the spray scrubber diameter, flue gas velocity, residence time and liquid flow per single spray bank are 7.0 m, $3.5 \text{ m} \cdot \text{s}^{-1}$, 2 s and $480.0 \text{ m}^3/\text{h}$, respectively. The coal consumption of the two boilers is 43.75 t/h and the sulfur content of the coal is about 1.0%. The design value of desulfurization efficiency of this ammonia-based wet flue gas desulfurization system is 95%.

The pH of the solution was monitored by automatic control systems. The inlet SO_2 concentration and outlet SO_2 concentration of the spray scrubber were measured by continuous emission monitoring systems. The protocol used for determining the measurement point in the duct is The Determination of Particulates and Sampling Methods of Gaseous Pollutants Emitted Gas of Stationary Source (Industry Standard DL/T467-2004).

RESULTS AND DISCUSSION

1. The Effect of pH

The effect of pH of scrubbing liquid on the SO_2 removal efficiency is shown in Fig. 3. It is obvious that the calculated values of SO_2 removal efficiency increase as the pH value increases. There is a close correspondence observed between the measured values (points) and the calculated ones (line). An examination of Fig. 3 also shows that the SO_2 removal efficiency increased quickly with the pH up to 5.5, above which it increased slowly.

As shown in Eq. (2), SO_2 was absorbed mainly by reacting with $(\text{NH}_4)_2\text{SO}_3$ in the solution. It can be seen from Fig. 2 that the distribution coefficient of SO_3^{2-} increases as the pH increases. Accordingly, the SO_2 removal efficiency increases with the pH. The distribution coefficient of SO_3^{2-} is 2.17×10^{-2} at pH 5.7 and it drops from

Table 1. Values of model parameters

Parameters	Value
H ($\text{kmol} \cdot \text{m}^{-3} \cdot \text{Pa}^{-1}$)	6.38×10^{-3}
μ_g ($\text{Pa} \cdot \text{s}$)	1.95×10^{-5}
M_{air} ($\text{g} \cdot \text{mol}^{-1}$)	29
M_{SO_2} ($\text{g} \cdot \text{mol}^{-1}$)	64
V_{air} ($\text{cm}^3 \cdot \text{mol}^{-1}$)	20.1
V_{SO_2} ($\text{cm}^3 \cdot \text{mol}^{-1}$)	41.1
K_{hc}	79.73
K_c	1.8×10^{-5}
K_w	5.58×10^{-14}
K_{ha}	5.4×10^{-6}
K_{a1}	7.94×10^{-3}
K_{a2}	4.4×10^{-8}
T (K)	323.15 K
p (Pa)	101325

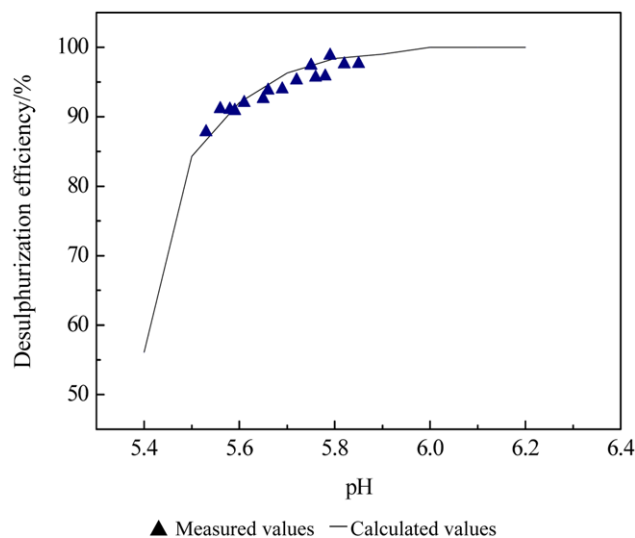


Fig. 3. The effect of pH ($G=456120.3 \text{ m}^3 \cdot \text{h}^{-1}$; $C_{\text{SO}_2}=2072.24 \text{ mg} \cdot \text{m}^{-3}$; $L/G=3.0$).

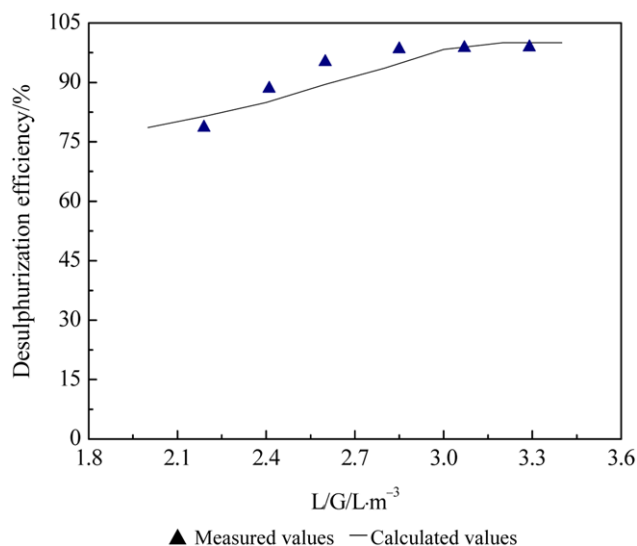


Fig. 4. The effect of liquid/gas ratio ($G=456120.3 \text{ m}^3 \cdot \text{h}^{-1}$; $C_{\text{SO}_2}=2072.24 \text{ mg} \cdot \text{m}^{-3}$; $\text{pH}=5.8$).

1.38×10^{-2} to 4.41×10^{-3} when the pH drops from 5.5 to 5.0. The distribution coefficient of SO_3^{2-} is nearly zero when the pH is below 5.0. Thus, the SO_2 removal efficiency drops drastically when the pH is below 5.5.

2. The Effect of Liquid-gas Ratio

The liquid-gas ratio plays an important role in the desulfurization process. The effect of liquid-gas ratio on SO_2 removal efficiency is shown in Fig. 4. Obviously, the calculated values agree well with the measured values. The response to an increasing liquid-gas ratio is obviously a higher SO_2 removal efficiency. It can be seen from the figure that the percentage removal of SO_2 initially increased rapidly with the increase in liquid-gas ratio and thereafter reached an almost constant value beyond a liquid-gas ratio of $3 \text{ L} \cdot \text{m}^{-3}$. The reason for such observation may be explained as follows: with the increase in the liquid-gas ratio, the liquid flow increased, and as the liquid flow rate increased, the total droplet surface area was also increased. Accordingly, the percentage of removal of SO_2 increased with the increase in liquid-gas ratio. The percentage removal of SO_2 remained almost constant beyond a liquid-gas ratio of $3 \text{ L} \cdot \text{m}^{-3}$, which could mainly be due to the fact that SO_2 concentration in the flue gas was reaching its equilibrium value. It could also be due to the result that the coalescence of the droplets increased with the liquid-gas ratio up to $3 \text{ L} \cdot \text{m}^{-3}$, whereby the total droplet surface area might decrease and the SO_2 removal efficiency level off. A similar tendency has also been observed by Huang and Amitava [20,21].

3. The Effect of Flue Gas Velocity

The model was used to simulate the process of SO_2 absorption at various flue gas velocities, and the calculated desulfurization efficiency is plotted in Fig. 5. It is evident that the SO_2 removal efficiency is inversely proportional to the flue gas velocity. The calculated SO_2 removal efficiency decreases from 96.77% to 94.06% when the flue gas velocity increases from $3.6 \text{ m} \cdot \text{s}^{-1}$ to $4.0 \text{ m} \cdot \text{s}^{-1}$. A rise in flue gas velocity results in a decreasing gas residence time. Accordingly, the desulfurization efficiency decreases as the flue gas velocity increases. Moreover, the amount of the entrained liquid droplets increases as the flue gas increases. It can be concluded that the spray

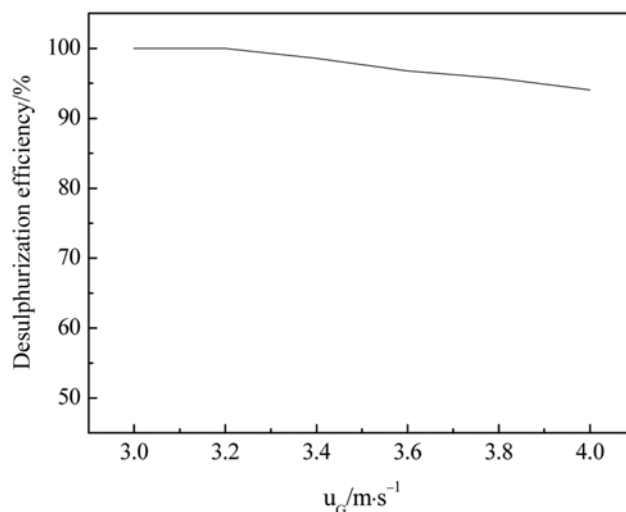


Fig. 5. The effect of flue gas velocity ($C_{\text{SO}_2}=2072.24 \text{ mg} \cdot \text{m}^{-3}$; $\text{pH}=5.8$; $L/G=3.0$).

scrubber should not be operated at the high value of the flue gas velocity.

The experiments were carried out with little change in flue gas velocity when the boiler was in normal operation. Accordingly, the calculated values for the operating conditions of flue gas velocity have not been compared with the experimental values. Further research is needed.

4. The Effect of SO_2 Concentration

Fig. 6 illustrates the influence of the SO_2 concentration on desulfurization efficiency. Experimental results are presented together with the calculated results. Obviously, the desulfurization efficiency decreases with the increase of SO_2 concentration and the agreement is satisfactory.

An examination of Fig. 6 shows that when the SO_2 concentration increases from $2,000 \text{ mg} \cdot \text{m}^{-3}$ to $4,000 \text{ mg} \cdot \text{m}^{-3}$, the calculated desulfurization efficiency decreases from 99.98% to 62.27%. The

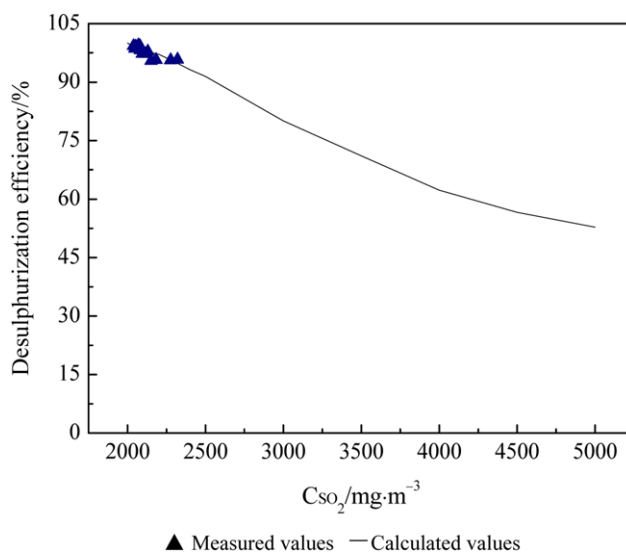


Fig. 6. The effect of SO_2 concentration ($G=456120.3 \text{ m}^3 \cdot \text{h}^{-1}$; $\text{pH}=5.8$; $L/G=3.0$).

reason may be that the absorbent in the solution cannot meet the chemical equivalent when the SO_2 concentration is $4,000 \text{ mg}\cdot\text{m}^{-3}$. To meet the SO_2 emission standard of flue gas in power plants, the structure of the spray scrubber or the operating parameters (e.g., pH and liquid-gas ratio) should be adjusted when the SO_2 concentration is too high.

CONCLUSIONS

Based on double-film theory, a mathematical model of ammonia-based wet flue gas desulfurization was developed to simulate the desulfurization process in spray scrubbers. This developed model includes the following operating parameters: pH, liquid-gas ratio, flue gas velocity and SO_2 concentration. The modeled results are compared with the measured results of an ammonia-based wet flue gas desulfurization system, which is used in a petrochemical works in Northwest China. The calculated values for the operating conditions of pH, liquid-gas ratio and SO_2 concentration closely correspond to the experimental values. The calculated results show that the desulfurization efficiency decreases as the flue gas velocity increases. In the present investigation, the experiments were carried out with little change in flue gas velocity when the boiler was in normal operation. Further experiments are needed for comparison with the calculated desulfurization efficiency for the operating condition flue gas velocity.

ACKNOWLEDGEMENTS

This work is supported by Natural Science Foundation of Jiangsu Province (No. BK2008421) and Jiangsu Heyichang Environmental Engineering & Technology Co., Ltd.

NOMENCLATURE

u^0 : initial Resultant velocity
 a : contact area in a element [m^2]
 C : concentration of ammonium ion [mol/L]
 C_{drag} : drag coefficient
 D_{SO_2} : diffusion coefficient of SO_2 [m^2/h]
 d_p : diameter of liquid drop [m]
 G : volumetric gas flow rate [kmol/h]
 g : acceleration of gravity [m/s^2]
 K_{a1} : chemical equilibrium constant
 K_{a2} : chemical equilibrium constant
 K_C : chemical equilibrium constant
 K_{ha} : chemical equilibrium constant
 K_{hC} : chemical equilibrium constant
 K_W : ion-product constant of water
 k_y : gas-phase mass transfer coefficient [$\text{kmol}/(\text{m}^2\cdot\text{h})$]
 L : liquid flow rate [m^3/h]
 M : molar flow rate of total sulfur [kmol/h]
 M_{air} : molar mass of air [g/mol]
 M_{SO_2} : molar mass of SO_2 [g/mol]
 N : constant
 p : total pressure of flue gas [Pa]
 $P_{\text{SO}_2}^*$: equilibrium partial pressure of SO_2 [Pa]
 $P_{\text{SO}_2,o}^*$: equilibrium partial pressure of SO_2 at the top of absorption

zone [Pa]
 $P_{\text{NH}_3}^*$: equilibrium partial pressure of NH_3 [Pa]
 R : gas constant [$8.31 \text{ J}/(\text{mol}\cdot\text{K})$]
 Re : Reynolds number
 S : concentration of total sulfite [mol/L]
 Sc : Schmidt number
 Sh : Sherwood number
 T : temperature [K]
 t : time [min]
 t_z : the time of the liquid pass through the incremental volume [m/s]
 u_p^0 : initial velocity of droplets [m/s]
 u_p : droplets velocity with respect to the scrubber wall [m/s]
 u_g : flue gas velocity with respect to the scrubber wall [m/s]
 V_{air} : molecular volume of air [cm^3/mol]
 V_{SO_2} : molecular volume of SO_2 [cm^3/mol]
 y : mole fraction of SO_2
 y_1 : inlet mole fraction of SO_2
 y_2 : outlet mole fraction of SO_2
 y_i : equilibrium mole fraction of SO_2
 Z : the arbitrary height from the top of scrubber [m]
 Z_T : the height of the absorption zone [m]
 $[\text{H}^+]$: concentration of hydrogen ion [mol/L]
 $[\text{H}^+]_0$: initial hydrogen ion concentration at the top of scrubber [mol/L]
 $[\text{HH}_4^+]$: concentration of bisulfate ion [mol/L]
 $[\text{HSO}_3^-]$: concentration of ammonium ion [mol/L]
 $[\text{OH}^-]$: concentration of hydroxide ion [mol/L]
 $[\text{SO}_3^{2-}]$: concentration of sulfite ion [mol/L]
 $[\text{SO}_4^{2-}]$: concentration of sulfate ion [mol/L]

Greek Letters

η : SO_2 removal efficiency [%]
 λ : turbulence length scale [m]
 λ_0 : distribution coefficient of H_2SO_3
 λ_1 : distribution coefficient of HSO_3^-
 λ_2 : distribution coefficient of SO_3^{2-}
 μ_g : viscosity of flue gas [$\text{Pa}\cdot\text{s}$]
 ρ_g : density of gas [kg/m^3]
 ρ_p : the density of solution [kg/m^3]

Subscript

b : the bottom of the absorption zone
 in : flow into
 out : flow out
 Z : any cross section of the absorption zone

REFERENCES

1. D. Thomas, S. Colle and J. Vanderchuren, *Chem. Eng. Process.*, **42**, 487 (2003).
2. S. Colle, D. Thomas and J. Vanderschuren, *Chem. Eng. Res. Des.*, **83**, 81 (2005).
3. B. S. He, X. Y. Zheng, Y. Wen, H. L. Tong, M. Q. Chen and C. H. Chen, *Energy Convers. Manage.*, **44**, 2175 (2003).
4. J. Warych and M. Szymanowski, *Ind. Eng. Chem. Res.*, **40**, 2597 (2001).

5. J. Warych and M. Szymanowski, *Chem. Eng. Technol.*, **25**, 427 (2002).
6. J. C. Sai, S. H. Wu, R. Xu, R. Sun, Y. Zhao and Y. K. Qin, *Korean J. Chem. Eng.*, **24**, 481 (2007).
7. Y. Zhong, X. Gao, W. Hou, Z. Y. Luo, M. J. Ni and K. F. Cen, *Fuel Process. Technol.*, **89**, 1025 (2008).
8. A. Saleem, US Patent, 4,690,807 (1987).
9. A. Saleem, E. Gal, G. Brown and M. M. Fredericksburg, US Patent, 5,362,458 (1994).
10. D. C. Borio, D. J. Muraskin, P. C. Rader and M. A. Waters, US Patent, 6,531,104 B1 (2003).
11. X. Gao, H. L. Ding, Z. Du, Z. L. Wu, M. X. Fang, Z. Y. Luo and K. F. Cen, *Appl. Energ.*, **87**, 2647 (2010).
12. Y. X. Guo, Z. Y. Liu, Z. G. Huang, Q. Y. Liu and S. J. Guo, *Ind. Eng. Chem. Res.*, **44**, 9989 (2005).
13. H. F. Johnstone, *Ind. Eng. Chem.*, **29**, 1396 (1937).
14. P. K. Wu, L. K. Tseng and G. M. Faeth, *Atomization Sprays*, **2**, 295 (1995).
15. C. Brogren and H. T. Karlsson, *Chem. Eng. Sci.*, **52**, 3085 (1997).
16. Q. Wu, *The engineering of mass transfer and separate*, South China University of Technology Press. Publications, Guangzhou (2005).
17. G. M. Xiang, *Studied of slurry jet flue gas desulfurization*, Ph. D. Tsinghua University, Beijing (2003).
18. J. A. Michalski, *Ind. Eng. Chem. Res.*, **39**, 3314 (2000).
19. M. Doumas, *Chem. Eng. Prog.*, **49**, 518 (1953).
20. C. H. Huang, *J. Environ. Sci. Health., Part A.*, **40**, 2027 (2005).
21. B. Amitava and N. B. Manindra, *Chem. Eng. J.*, **139**, 29 (2008).